International Journal of Microwave and Wireless Technologies

cambridge.org/mrf

Site and orbital diversity prediction at Ka/Q bands for high throughput satellite systems in South Eastern Europe

Nektarios Moraitis[1], Apostolos Z. Papafragkakis[1], Athanasios D. Panagopoulos[1], Panayiotis Ioannides[2], Nikolaos Christoforou[2], Constantinos Agrotis[2] and Sotirios Alexandrou[2]

[1]School of Electrical and Computer Engineering, National Technical University of Athens, Athens, Greece and [2]Cyprus Telecommunications Authority (Cyta), Kakoradjia, Kofinou, Larnaca, Cyprus

Research Paper

Cite this article: Moraitis N, Papafragkakis AZ, Panagopoulos AD, Ioannides P, Christoforou N, Agrotis C, Alexandrou S (2026) Site and orbital diversity prediction at Ka/Q bands for high throughput satellite systems in South Eastern Europe. *International Journal of Microwave and Wireless Technologies*, 1–11. https://doi.org/10.1017/S1759078726102852

Received: 11 September 2025
Revised: 30 December 2025
Accepted: 31 December 2025

Keywords:
high throughput satellites (HTS); orbital diversity; rainfall rate; site diversity

Corresponding author: Nektarios Moraitis; Email: morai@mobile.ntua.gr

Abstract

This article examines the benefits of utilizing site and orbital diversity reception techniques at Ka- and Q-bands in South Eastern Europe, comparing their performance in Cyprus and Greece. The assessment relies on measured rainfall rate statistics, collected near the selected locations in both countries. The study compares and evaluates the performance of double and triple site and orbital diversity scenarios. The simulation outcome reveals that the adoption of double and triple site, or double and triple orbital diversity configurations leads to considerable enhancements in outage performance in both frequency bands. The delivered improvements are markedly significant when specifically 3-site and 3-orbit diversities are applied, especially at Q-band. However, the orbital diversity demonstrates inferior performance compared with site diversity. Notably, for satellite systems demanding extremely high levels of service continuity, the 3-site diversity approach proves highly effective at Ka- and Q-bands, accomplishing this without necessitating overly large fade margins. Comparing Cyprus and Greece, the latter demonstrates lower outage improvements due to the higher measured rainfall rates. Finally, for a dual orbital diversity scenario in Greece, measured experimental results are presented in terms of joint attenuation and compared with the theoretical model, exhibiting noticeable accuracy.

Introduction

An earlier version of this paper was presented at the 19th Conference on Antennas and Propagation (EuCAP2025) and was published in its Proceedings [1].

High throughput satellites (HTS) are expected to achieve data rates up to terabit-per-second (Tb/s), which demands significant amount of spectrum allocation [2]. To meet these requirements, contemporary satellite systems leverage new frequency allocations at Ka- and Q-bands and taking advantage of the broad usable bandwidth would be able to accommodate advanced services with enhanced transmission rates. However, operating at these frequencies exposes satellite links to pronounced atmospheric impairments, especially the extreme rainfall rate events, which can introduce substantial signal attenuation and degrade the satellite links performance and quality of service [3], [4]. Furthermore, the European Union's new secure satellite internet constellation IRIS2 has been employed in [5], whereas a new stochastic model for site and orbital diversity reception schemes has been introduced in [6]. In [7], the ground segment design for Q/V band is studied for NGSO satellite systems, and finally, the rain fronts effects on site diversity techniques in Ku-band are studied in [8].

To counteract these adverse atmospheric effects, a variety of fade mitigation techniques (FMTs) may be adopted to meet the required quality-of-service (QoS) criteria imposed by the services, and in parallel, maintain an optimal level of resource usage [9]. The main concept behind FMTs is to reconfigure the earth-space link and improve the overall availability, thereby sustaining a tolerable throughput limit during a rain event. They leverage the non-uniform spatial and temporal nature of those propagation phenomena by changing features involved in the link budget or the baseband signal and compensate for the signal attenuation. The most common FMTs, proposed for Ka-band and above, include adaptive coding and modulation (ACM), reconfigurable antennas onboard the satellite, adaptive power control (APC), frequency diversity, time diversity, site diversity, and orbital diversity [10]. However, many of those approaches, often entail stringent hardware investments, intricate system design and increase resource usage, thus limiting in practice their widespread deployment. Consequently, site diversity is

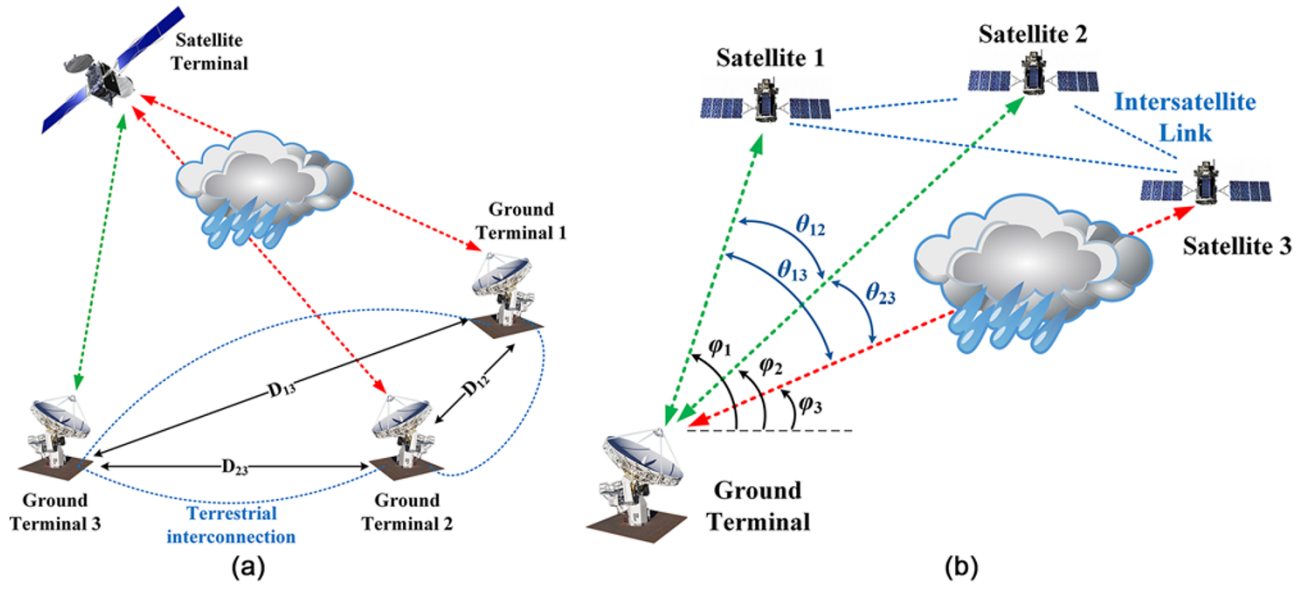

Figure 1. Indicative paradigm of the examined diversity scenarios. (a) Triple-site diversity. (b) Triple-orbital diversity.

frequently exploited due to its effectiveness in alleviating the rain-induced attenuation. This technique involves connecting two or more geographically separated ground stations, taking advantage of the spatial variability of rainfall. Given that the rain rate correlation reduces with increasing separation between ground terminals, switching to the location with the strongest received signal, or with the lowest attenuation, will drastically decrease precipitation-related impairments (i.e., applying proper selection combining techniques). The success of site diversity is based on the low spatial correlation between the slant paths involved.

Alike site diversity method, orbital or satellite diversity exploits the spatial variability of the rain medium by pointing the ground station antenna to various satellites, thus altering the slant path. For this purpose, a different antenna can be utilized, or the same, provided that it is supported by a fast-acquisition tracking system. It should be pointed out that the satellites should preserve a line-of-sight (LOS) path with the ground terminal and be able to convey the information between them, either by inter-satellite link with the master satellite, or having multiple antennas/tracking system at the ground station to adapt pointing to the satellites. Orbital diversity is in essence a reversed site diversity, although it is anticipated to have inferior performance as the alterative slant paths are not sufficiently uncorrelated. Consequently, the higher the angular separation between the satellites, the higher the achievable gain [11]. It is a more economically feasible solution, as a sole ground station needs to be used, nonetheless, it requires a system controller that can result in delay upon satellite switching/traffic rerouting if a single antenna is used. Moreover, it requires to double or triple the capacity bandwidth from the satellites. The conceptual layouts of a triple-site and triple-orbital diversity scenarios are illustrated in Fig. 1.

In this context, it is fundamental to analyze, assess, and validate the performance of such diversity schemes exploiting local experimental data and theoretical modeling prior to earth station deployment. The role of local rain measurements is also highlighted in [1], indicating that those are preferable conveying more accurate information about the rain statistics. In some cases, solely dual-site diversity may not effectively diminish fade margins or guarantee robust link availability [10, 12]. Therefore, the adoption of triple-site diversity schemes becomes a necessity. The same stands for orbital diversity [13].

This work extends the study in [1] and presents the enhancement in outage performance afforded by triple site and orbital diversity configurations, leveraging a theoretical framework based on the lognormal distribution for local rainfall rates, modeling rain attenuation over individual slant paths. The introduced approach considers the joint tri-variate Lognormal distribution to characterize rain-induced signal fading across three slant paths in the triple site diversity scheme, where inter-terminal correlation is modeled by the convective rain cell approach for distances under 50 km and the ITU-R Paraboni–Barbaliscia formula for longer distances [14], [15]. The applied model is a combination in terms of correlation dependence, of convective rain cell method for distances below 50 km, and, for distances above 50 km, the ITU-R P.618 expression is employed. The model for distances below 50 km has been efficiently tested and validated, in numerous research studies in the past with great success [16], [17], [18]. For the orbital diversity the inter-satellite correlation is modeled solely by the convective rain cell method. The foundational models for double and triple site diversity were initially introduced in related works in[16] and [17], while recent advances have extended these principles to multi-site diversity prediction [18]. A general time-series generator model for multi-slant paths has been proposed in [19]. The time-series prediction models can be effectively leveraged for the evaluation of multiple site and orbital diversity schemes. A theoretical model for orbital diversity has been studied in [20], comparing the results with site diversity. The triple orbital diversity method has been proposed and studied theoretically in [13]. Experimental results for orbital diversity scenarios have been carried out in [21]. Finally, orbital and spatial diversity have been proposed as fade countermeasures for next-generation large NGSO satellite constellations [22].

The aim of this study is to simulate and evaluate the performance of a site diversity scheme for three locations across Cyprus

https://doi.org/10.1017/S1759078726102852 Published online by Cambridge University Press

where Cyta operates teleports serving various frequency bands and satellites. The performance of the triple site diversity is also compared with Greece where two ground terminals are established for experimental measurements in Attica, and one additional location of existing teleport facilities. Furthermore, a triple orbital diversity scenario is also evaluated for both territories having a single master station pointing at different satellites. The entire analysis is supported by local experimental meteorological measurements, consisting of long-term rainfall intensity records for specific sites in both countries. This work presents the first analytical investigation of a triple-site and triple-orbit diversity reception schemes in the Ka-and Q-bands comparing two different territories and assisted by local rainfall data. Finally, the performance of a dual orbital satellite scenario is compared with the theoretical model predictions. The results aim to assist in the implementation of a practical solution for enhancing the performance of the local provider's satellite services. Comparative analyses demonstrate the significant advantages of leveraging triple-site and triple-orbital diversity over conventional single-site/orbit reception in mitigating rain-induced outages and improving service availability.

The rest of the paper is outlined as follows. The theoretical approach for the triple-site and orbit diversity schemes for the rain attenuation is described analytically in Section II. The examined scenarios in Cyprus and Greece, as well as important information about the rainfall measurements, are presented in Section III. The diversity performance comparing both territories is assessed in Section IV, delivering valuable numerical results and statistics. Finally, interesting conclusions are drawn in Section V, along with future steps.

Theoretical background

Site diversity

Satellite systems that operate at 10 GHz and above, the most dominant factor that affects signal degradation is rain. Consequently, the channel model for the slant paths prioritizes the impact of rain-induced fading. The key points for the statistical characterization of such channel models take into consideration the following remarks.

- The statistical analysis is based on the convective raincells model [16].
- The unconditional Lognormal distribution is used to approximate the random variables of the rain attenuation A (given in decibels) and the rainfall rate R (given in mm/h). The term unconditional point rainfall rate is determined as comprising both raining and non-raining events.
- To determine the mean and standard deviation features of the rainfall rate a fitting procedure is performed to the local measured data. If these are not available, the rain rates are determined by using ITU-R Recommendation P.837-7 [23].
- The rain heights (required for each slant path) are extrapolated leveraging ITU-R Recommendation P.839-4 [24].
- Regarding the homogeneity of the vertical structure of the rainfall medium, Crane's hypothesis has been considered [25]. In this case, the rain attenuation over the earth projection of a slant path A is associated with the rain attenuation A_s over the slant path according to $A = A_s \cos\phi$, where ϕ is the elevation angle.

The spatial correlation coefficient of the specific rain attenuation attributes is expressed as

$$\rho_0(d) = \begin{cases} \frac{G}{\sqrt{G^2+d^2}}, & d \le D_r \\ \frac{G}{\sqrt{G^2+D_r^2}}, & d > D_r \end{cases} \tag{1}$$

where D_r stands for the diameter of the raincell and G indicates the spatial factor of the rainfall medium $G \in [0.75, 3]$ that specifies the spatial correlation. The *logarithmic* correlation coefficient of the rain attenuation for $d \le 50$ km is given by

$$\rho_{n_{ij}} = \frac{1}{S_{a_i} S_{a_j}} \ln\left(1 + \rho_{ij}\sqrt{(e^{S^2_{a_i}} - 1)(e^{S^2_{a_j}} - 1)}\right) \tag{2}$$

where $i, j = 1, 2, 3$ $(i \neq j)$. Furthermore, $S^2_{a_i}$, $(i = 1, 2, 3)$, stands for the variance that depends on the rainfall rate statistics, which is expressed as

$$S^2_{a_i} = \ln\left(1 + \frac{H_{1i}}{L^2_{D_i}}\left[\exp\left(b_i^2 S^2_{r_i}\right) - 1\right]\right) \tag{3}$$

where b_i, $(i = 1, 2, 3)$, denotes the polarization and frequency dependent attenuation parameter, and S_{r_i} is a lognormal statistical parameter that is extrapolated from rainfall rate distribution R (see Fig. 3). Furthermore, H_{1i} indicates the effective height of the rainfall structure and L_{D_i} stands for the effective path length for the i-th slant path $(i = 1, 2, 3)$.

In the case of $d > 50$ km, then, the Paraboni–Barbalisca model is adopted according to

$$\rho_{n_{ij}} = 0.94 \exp\left(-\frac{d}{30}\right) + 0.06 \exp\left(-\left(\frac{d}{500}\right)^2\right) \tag{4}$$

In (2), ρ_{ij} is the correlation coefficient factor that is calculated by

$$\rho_{ij} = \frac{H_{2ij} = \int_0^{L_{D_i}} \int_0^{L_{D_j}} \rho_0(z, z')\, dz\, dz'}{\sqrt{H_{1i} H_{1j}}} \tag{5}$$

where z and z' denote the integral's argument features that are associated with the i-th and j-th effective path length, and H_{1i} is given by

$$H_{1i} = \begin{cases} 2L_{D_i} G \sinh^{-1}\left(\frac{L_{D_i}}{G}\right) + 2G^2\left(1 - \sqrt{\left(\frac{L_{D_i}}{G}\right)^2 + 1}\right), & L_{D_i} \le D_r \\ 2L_{D_i} G \sinh^{-1}\left(\frac{D_r}{G}\right) + 2G^2\left(1 - \sqrt{\left(\frac{D_r}{G}\right)^2 + 1}\right) & \\ \quad + \frac{G(L_{D_i} - D_r)^2}{\sqrt{G^2 + D_r^2}}, & L_{D_i} > D_r \end{cases} \tag{6}$$

The same stands for H_{1j} where $i, j = 1, 2, 3$ $(i \neq j)$. The features indicated in (1)–(6) and the annotations of the effective lengths L_{D_i}, given in kilometers, are available in [26, 27].

The improvement, achieved by the triple site diversity scenario, is assessed by determining the joint probability $P_{1,2,3}$. The latter parameter is expressed in terms of either the single-site probability at the relevant location, or by using the geometric mean probability P_0 of the P_1, P_2, and P_3 according to [16]

$$\begin{aligned} P_{1,2,3} &= P[A_{s1} > x_s, A_{s2} > x_s, A_{s3} > x_s] \\ &= P[A_1 > x_D, A_2 > x_D, A_3 > x_D] \\ &= \int_{x_D}^{\infty} \int_{x_D}^{\infty} \int_{x_D}^{\infty} f_{A_1 A_2 A_3}(x_1, x_2, x_3)\, dx_1\, dx_2\, dx_3 \end{aligned} \tag{7}$$

where $f_{A_1 A_2 A_3}(x_1, x_2, x_3)$ is the joint density function of the attenuation features A_1, A_2 and A_3. Given that the random variables $\ln A_1$,

https://doi.org/10.1017/S1759078726102852 Published online by Cambridge University Press

$\ln A_2$, and $\ln A_3$ approximate a joint unconditional normal distribution, applying a straightforward statistical analysis, the triple site probability can be determined according to

$$P_{1,2,3} = \frac{1}{2}\int_{u_0}^{\infty}\int_{u_0}^{\infty} f_{U_2U_3}(u_2,u_3)\mathrm{erfc}\left(\frac{u_0-m_1}{\sqrt{2}\sigma_1}\right)du_2\,du_3 \quad (8)$$

where $f_{U_2U_3}(u_2,u_3)$ is the bivariate normal density distribution that is described by

$$f_{U_2U_3}(u_2,u_3) = \frac{1}{2\pi\sqrt{1-\rho_{n_{23}}^2}}\exp\left(-\frac{u_2^2+u_3^2-2\rho_{n_{23}}u_2u_3}{2(1-\rho_{n_{23}}^2)}\right) \quad (9)$$

and $u_0 = \sqrt{2}\mathrm{erfc}^{-1}(2P_0)$. The variable m_1 and σ_1 are expressed as

$$m_1 = \frac{(\rho_{n_{12}}-\rho_{n_{13}}\rho_{n_{23}})u_2 + (\rho_{n_{13}}-\rho_{n_{12}}\rho_{n_{23}})u_3}{1-\rho_{n_{23}}^2} \quad (10)$$

$$\sigma_1 = \left[\frac{(1-\rho_{n_{12}}^2-\rho_{n_{23}}^2-\rho_{n_{13}}^2+2\rho_{n_{12}}\rho_{n_{23}}\rho_{n_{13}})}{1-\rho_{n_{23}}^2}\right]^{\frac{1}{2}} \quad (11)$$

and the parameter u_i, is expressed as

$$u_i = \frac{\ln A_i - \ln A_{m_i}}{S_{a_i}},\ i=1,2,3 \quad (12)$$

where $S_{a_i}^2$, $(i=1,2,3)$, is given by (3) and A_{m_i} is determined by

$$A_{m_i} = a_i R_{m_i}^{b_i} L_{D_i}\exp\left(\frac{b_i^2 S_{r_i}^2 - S_{a_i}^2}{2}\right) \quad (13)$$

where a_i, $(i=1,2,3)$, stands for the polarization and frequency dependent attenuation parameter, and S_{r_i} is a lognormal statistical parameter that determined by the rainfall rate distribution R. The parameters A_{m_i} and $S_{a_i}^2$ are the statistical attributes of the induced rain attenuation (given in decibels) in each slant path, thereby facilitating the triple site diversity method. It should be pointed out that the probability given by (8) is grounded on the selection combining method, thus outage is represented by (7).

Orbital diversity

The general configuration of the orbital diversity scenario with three geostationary satellites is shown in Fig. 1(b), where φ_1, φ_2, φ_3 are the elevation angles of each slant path. The objective is to determine the service availability improvement using triple-orbital diversity, which is addressed by calculating the exceedance probability given by (6). In essence, the theoretical model presented above can be reversed and instead of having three ground stations, three different satellites, linked to a single ground station, are exploited to improve the performance. The system moderator switches and selects the satellite with the lower attenuation level. Therefore, the required quality is realized with much smaller available link margin from the corresponding one that we have for a single- or double-orbital diversity layout for the same time availability. The difference with the triple site diversity is grounded on the calculation of the correlation coefficient ρ_{ij}. In (5), to calculate H_{2ij}, the spatial correlation coefficient in the nominator is expressed as

$$\rho_0(z,z') = \frac{G}{\sqrt{G^2+d(z,z')^2}} \quad (14)$$

where $d(z,z') = \sqrt{z^2+z'^2-2zz'\Delta\psi_{ij}}$ is the distance between two points belonging to the projections of the slant paths under consideration, whereas the angle $\Delta\psi_{ij}$, $i,j=1,2,3$ $(i\neq j)$, is given by

$$\Delta\psi_{ij} = \cos^{-1}\left((\cos\theta_{ij}-\sin\varphi_i\sin\varphi_j)/\cos\varphi_i\cos\varphi_j\right) \quad (15)$$

where θ_{ij} is the angular separation between two pairs of satellites as shown in Fig. 1(b), and φ is the elevation angle of the corresponding ground station antenna pointing to each satellite.

Diversity scenarios under consideration

In the island of Cyprus, the diversity scenario comprises two operating teleport terminals in Makarios and Pera. A third location is taken into account in the west part of the island (Pathos site) to aid the suggested triple site diversity concept. In Greece, the experimental terminals are located on the campus of the National Technical University of Athens (NTUA) and Lavrion Technological and Cultural Park (LTPC), respectively. The third site is selected in the Nemea Teleport, which serves the ground terminals of many providers. The corresponding locations and the direct path distance between them, for Cyprus and Greece, are depicted in Fig. 2(a) and (b), respectively.

The selected site coordinates for both countries are listed in Table 1. The geographical spacing between individual sites plays a key role in determining how well the diversity system performs. In Cyprus, the chosen locations of Makarios and Pera have a spatial separation of 22.6 km, with the eastern part of the Troodos mountain range intervening. Furthermore, the distances between Makarios-Paphos and Pera-Paphos are 87.5 km and 79.9 km, respectively. In Greece, the two main locations of NTUA and LTCP are separated about 36.4 km, whereas the Ymittos mountain creates a natural barrier between them. Accordingly, the separation distance between NTUA-Nemea and LTCP-Nemea is 103 and 126 km, respectively. Nemea teleport is deliberately located between many mountains to achieve a physical isolation from interference in a relatively dry area with low rain events. The created geographic barriers influence the development of the local weather conditions, which is highly likely to lead in higher diversity gains, as they improve the physical isolation between the teleports. The impact is expected to be even more noticeable, adding Paphos and Nemea ground terminals in Cyprus and Greece, respectively, which are both significantly more isolated compared with the other two. Establishing additional sites entails an increased cost of a diversity-based reception method. In this work, the selection of all sites is based on practical considerations (i.e., existing teleport locations or deployed experimental terminals). Conventionally, the choice of the ground stations relies on both climatic conditions and the geometric constraints/characteristics of potential locations [28]. It should be clarified that all the above comments would make sense if there were real experimental facilities to receive real measured data. In this paper, emphasis is given solely on simulated data from theoretical models that do not take into account the weather front in the assumed correlation dependence. There is an ongoing experimental campaign for site diversity reception measured data to prove the influence of the local geographical peculiarities in Greece and Cyprus.

https://doi.org/10.1017/S1759078726102852 Published online by Cambridge University Press

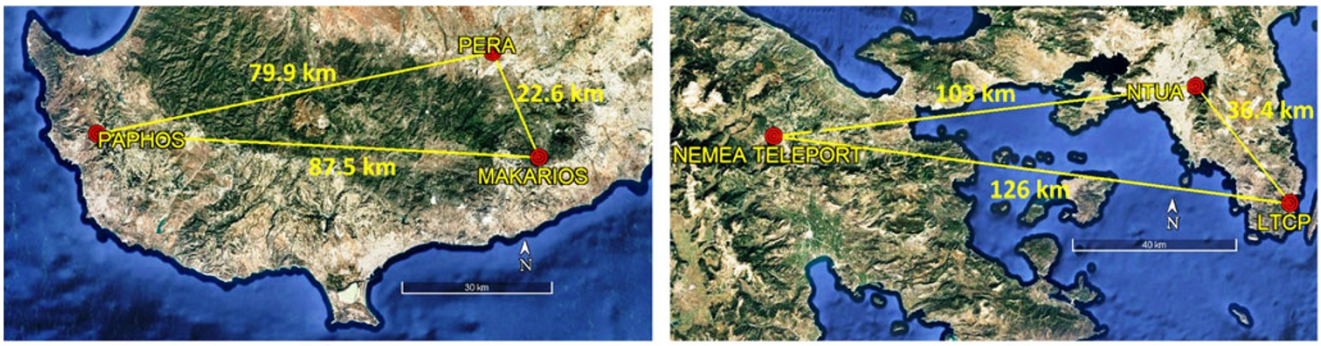

Figure 2. Indicative satellite pictures between the selected sites (taken from Google Earth™). (a) In Cyprus. (b) In Greece.

Table 1. Geographical coordinates of the examined locations in Cyprus and Greece

	Teleport	Makarios	Pera	Paphos
Cyprus	Latitude	34°51′37″N	35°02′50″N	34°54′06″N
	Longitude	33°22′56″E	33°16′59″E	32°25′34″N
	Altitude	222 m	373 m	643 m
	Teleport	NTUA	LTCP	Nemea
Greece	Latitude	37°58′32″N	37°43′29″N	37°50′43″N
	Longitude	23°47′06″E	24°03′05″E	22°37′26″N
	Altitude	220 m	10 m	277 m

In Cyprus, long-term experimental meteorological data were collected between 2016 and 2021, including rainfall intensity values locally for Makarios and Pera sites (taken from the Cypriot Meteo Organization), registered at 10-min intervals. In Greece, 4-year data was collected (2016-2020) at 10-min intervals, in both NTUA and LTCP locations (exploiting tipping buckets at each terminal). The data availabilities were 94.96%, 96.43%, 92.33%, and 99.87% for Makarios, Pera, NTUA, and LTCP locations, respectively. The collected data was of high quality as the recorded values maintain consistency with no discontinuities or surges, thereby acting as a reliable baseline feature to be employed in different simulated diversity scenarios enhancing accuracy. A well-established approach is adopted to transform the 10-minute rainfall measurements into corresponding 1-minute rainfall rates [29], which are then leveraged to obtain the point rainfall rate statistics necessary either for the simulations, or for various statistical/empirical attenuation models. The 1-min rate reveals clearly the dynamics of those raining events. For this purpose, the following conversion formula is utilized

$$R_{1\text{-min}}(p\%) = a \cdot R_{10\text{-min}}(p\%)^b \tag{16}$$

where $a = 0.829$ and $b = 1.097$ according to [30].

Figure 3 presents the related exceedance probability results versus rainfall rate for each selected location for Cyprus and Greece. Given that measured data is not available in Paphos and Nemea locations, these are extrapolated taking into account ITU rain-map database [23]. The attributes R_{m_i} and S_{r_i} required in (2) and (13) are determined from the measured data and the rain-maps. The results show that higher rain intensities are encountered in Greece compared with Cyprus locations. More specifically, NTUA and LTCP exhibit the highest rain rates with comparable plots. Another observation is that Makarios and Pera also deliver comparable rainfall rates. This could be probably credited to the rainfall characteristics, whose statistics are not expected to change drastically at relatively small territories, as shown in Fig. 2. However, discrepancies are observed between the measured rainfall properties and the corresponding calculations from ITU, especially in Greece if one compares NTUA and LTCP with Nemea plots. Therefore, for enhanced accuracy and credibility, the simulations should be based on local measured rainfall data, as also suggested in [1].

In the following procedure, vertical polarization is assumed. Furthermore, the selected frequencies are 20 GHz and 40 GHz at Ka- and Q-bands, respectively. In the case of the triple site diversity the selected elevation angles are 43.4° and 45.24° for Greece and 49.42° and 45.45° for Cyprus at Ka- and Q-bands, respectively, based on the associated satellites. Given the short relative distance between the sites and the geostationary orbit of the satellites, these angles are common at each selected ground terminal at Cyprus and Greece. The Makarios ground terminal in Cyprus and NTUA in Greece are considered and set as reference in both site and orbital diversity scenarios.

The performance of the orbital diversity depends on and is subject to limitations upon the availability of the satellites in orbit, and their angular separation. The greater the separation, the highest achievable diversity gain. The terminals of NTUA and Makarios are both considered to point at KaSAT (9°E), ALPHASAT (25°E), and HellasSat (36°E) satellites. Therefore, the angular separations θ_{ij}, are $\theta_{12} = 16°$, $\theta_{13} = 30°$ and $\theta_{23} = 11°$, respectively. The corresponding elevation angles $\varphi_{1,2,3}$ are 43.4°, 46.1°, 43.2° for NTUA and 42.3°, 49.1° and 49.5° for Makarios sites, respectively. Finally, for the rest of the parameters, it is assumed that $G = 1.5$ km, $D_r = 30$km and $H_r = 4.8$ km.

https://doi.org/10.1017/S1759078726102852 Published online by Cambridge University Press

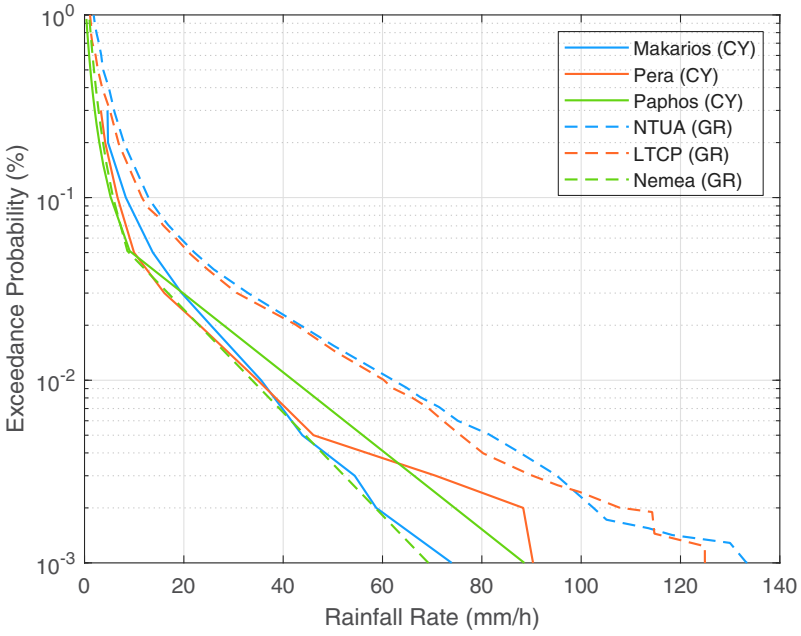

Figure 3. Exceedance probability versus rainfall rate for the locations under consideration.

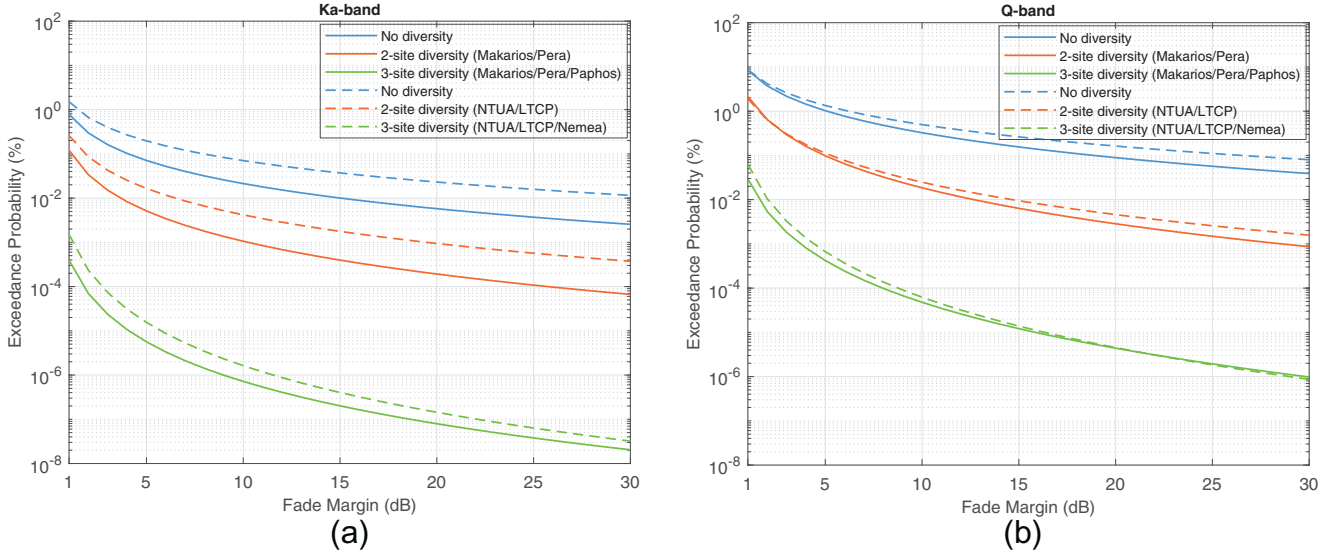

Figure 4. Comparison of site diversity performance between the selected sites in Cyprus and Greece. (a) Ka-band. (b) Q-band.

Performance evaluation

The exceedance probability (outage time) versus fade margin in the range of 1–30 dB is calculated at Ka- and Q-bands. Three cases are taken into account – no diversity, 2-site diversity, and 3-site diversity – and similarly, no diversity, 2-orbit, and 3-orbit diversity. The triple site diversity scenario is depicted in Fig. 4, comparing Cyprus and Greece territories.

It is evident that, in both cases, leveraging a 3-site diversity there is a remarkable improvement in exceedance probabilities and outage reduction, compared with 2-site diversity and no diversity. As expected higher frequencies induce higher attenuation that is reflected to the related outcome, as Q-band delivers inferior exceedance probabilities compared with Ka-band, as it clearly appears in the corresponding plots in Fig. 4(b) and (a), respectively. Comparing the results in Greece and Cyprus, the former exhibits markedly worser outages, consistently in the three examined cases (no diversity, 2-site, and 3-site). This is more intense at Ka-band where greater outage discrepancies are encountered. The higher rainfall rates in Greece and the greater separation of the selected sites account for these observations. On the other hand, smaller differences between Greece and Cyprus are encountered at Q-band according to Fig. 4(b). To assess quantitatively the performance of the applied site diversity scenarios the improvement factor between outage probabilities is introduced. The specific metric is defined by

$$I = \frac{P_b - P_a}{P_a} \times 100\% \tag{17}$$

where P_a and P_b denote the values between the examined exceedance probabilities for scenario a and b, respectively (i.e., the improvement between 2-site and no diversity or between 3-site and

https://doi.org/10.1017/S1759078726102852 Published online by Cambridge University Press

Table 2. Outage improvement comparing double and triple site diversity between Cyprus and Greece for 10 and 20 dB fade margin

		10 dB		20 dB	
		Cyprus	Greece	Cyprus	Greece
Ka-band	2-site	95.02%	94.06%	99.66%	95.92%
	3-site	99.93%	99.96%	99.96%	99.98%
Q-band	2-site	94.31%	95.01%	96.80%	97.18%
	3-site	99.74%	99.75%	99.85%	99.90%

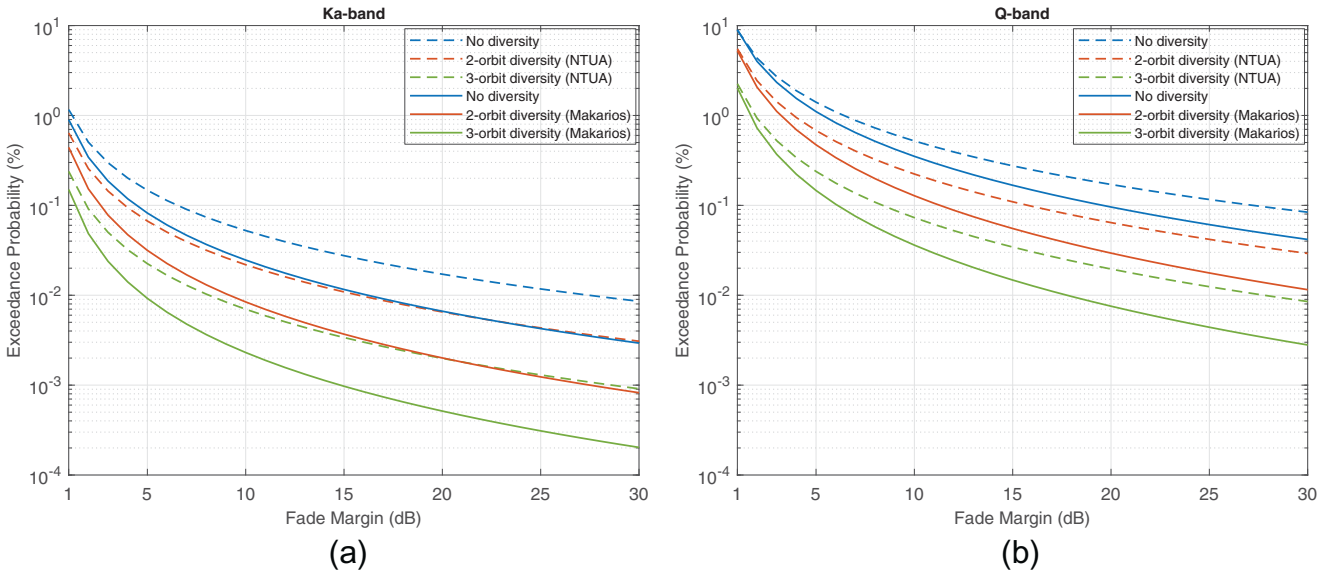

Figure 5. Comparison of orbital diversity performance between the selected sites in Cyprus and Greece. (a) Ka-band. (b) Q-band.

2-site diversity). The improvement factors for 10 and 20 dB fade margin are summarized in Table 2.

The numerical values reflect with consistency the previous remarks and the exceedance probabilities plots shown in Fig. 4. Obviously, the adoption of a 3-site diversity scenario delivers improvement factors higher than 99.9%, on average. The outage improvement between 2-site and 2-site diversity is about 4.5%, on average, for 10 dB fade margin at both frequencies and countries. Furthermore, the average improvements at Q-band are marginally better in Greece ($< 1\%$) as the separations between the selected sites are greater than those in Cyprus. On the other hand, Greece exhibits worser improvements than Cyprus at Ka-band, if 2-site diversity is applied (about 1% and 4.5% for 10 and 20 dB fade margins, respectively), due to the increased rainfall rates. Finally, the results indicated that 3-site diversity is indispensable at Q-band enhancing drastically the outage performance.

The results of the orbital diversity are presented in Fig. 5, in which 3-orbit diversity delivers the best outcome, improving substantially the system outage. The performance behavior between frequencies and countries is similar to the site diversity scenarios (i.e., deteriorated probabilities at Q-band and higher encountered outages in Greece). It is also apparent that site diversity outperforms orbital diversity, if one compares Figs. 4 and 5, which highlights the significance of the former technique that presents much better outages.

These observations are also evident in Table 3 where the numerical values of the outage improvement are summarized. Much lower values are obtained (between 57% and 74%) comparing the site and orbital diversity performance. However, in any case, the average improvement between 2-orbit and 3-orbit is about 7%, which is better than that in using 2-site and 3-site diversity (4.5%).

Furthermore, slightly better improvements are observed at Ka-band (7.5% on average) compared with Q-band (6.5% on average). The higher encountered rain rates in the NTUA location, compared with Makarios, are reflected to the improvement results, which according to Table 3, the former site presents, on average, about 5.5% deteriorated outages. It is also worth remarking that the discrepancies between NTUA and Makarios are more intense if a 2-orbit scenario is adopted (7% better outages for Makarios on average), instead of 3-orbit (4.6%), which suggests that the 3-orbit diversity compensates better the rain-induced attenuation improving the exceedance probabilities.

Orbital diversity real experiment in Athens

In the following, experimental attenuation results are presented solely at the NTUA location, where measurements are available at Ka-band, exploiting ALPHASAT (25°E) and KaSAT (9°E) satellites' beacon signal to evaluate orbital diversity. The measurements are then compared with the theoretical model for a 2-orbit exceedance probability. Figure 6 illustrates the measured diurnal in-excess attenuation versus time for two different days where rain events were encountered. The presented orbital diversity statistics are obtained after harmonizing the data to 1 sec time resolution, including only Ka-band attenuation data concurrent for both satellites. The differences in the recorded attenuation levels are more

https://doi.org/10.1017/S1759078726102852 Published online by Cambridge University Press

Table 3. Outage improvement comparing double and triple orbital diversity between Cyprus (Makarios) and Greece (NTUA) for 10 and 20 dB fade margin

		10 dB		20 dB	
		Cyprus	Greece	Cyprus	Greece
Ka-band	2-orbit	65.81%	58.32%	69.78%	61.99%
	3-orbit	72.63%	68.01%	74.37%	69.54%
Q-band	2-orbit	63.55%	57.13%	69.30%	62.35%
	3-orbit	71.77%	67.29%	74.33%	69.55%

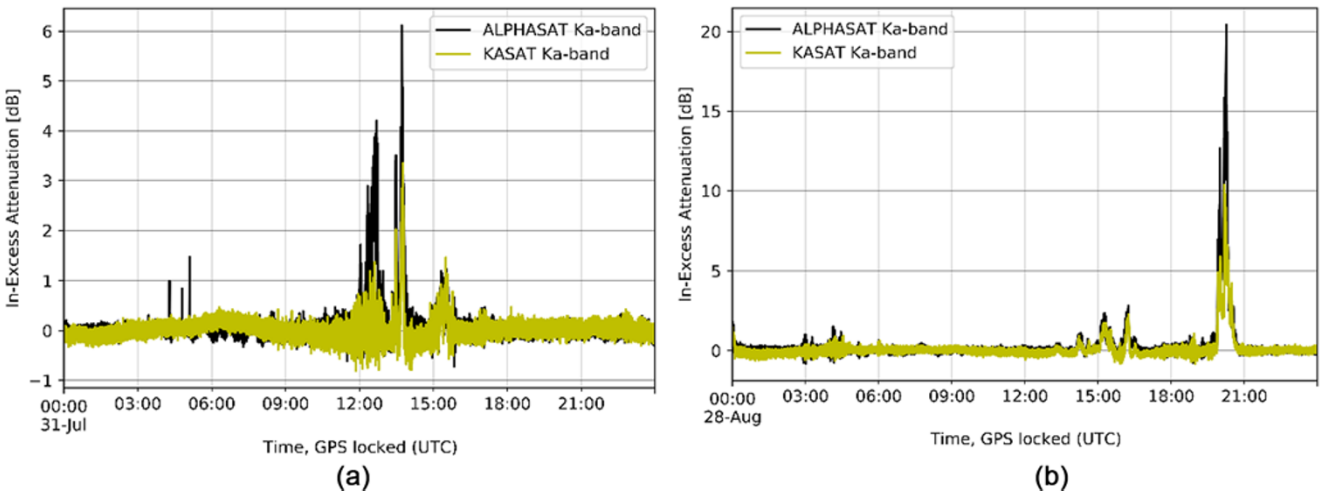

Figure 6. Example of the potential idealized orbital diversity technique for Ka-band at the NTUA location during two rainy days. (a) July 31st, 2023. (b) August 28th, 2023.

than evident between the two selected satellites, thus being favorable for adopting orbital diversity. The data have been processed according to the procedure described in [32] and [33]. According to Fig. 6, when intense rain events occur, the attenuation values differentiate between the two satellites, which can be leveraged for promising double orbital diversity gains.

The orbital diversity statistics for satellites at two orbital locations O_1 and O_2 are derived from the measured excess attenuation timeseries according to

$$P_{O_1,O_2} = \left[A_{O_1}(t) > a, A_{O_2}(t) > a\right] \tag{18}$$

where $P[\cdot]$ is the joint (bi-variate) probability complementary cumulative distribution function (CCDF) that attenuation values A_{O_1} and A_{O_2} at the time instant t exceed the attenuation threshold a. The ideal joint minimum attenuation experienced at time instant t is expressed as

$$A_{OD} = \min\left[A_{O_1}(t), A_{O_2}(t)\right] \tag{19}$$

The exceedance probability versus the measured joint excess attenuation for the double orbital scenario is presented in Fig. 7. The measured joint attenuation is in the range of 4–14.2 dB. It should be worth commenting that there is a slight frequency discrepancy between the two transmitted beacons as ALPHASAT transmits at 19.701 GHz with vertical polarization, while KaSAT at 19.680 GHz having horizontal polarization. Nevertheless, one can still obtain a good indication of the performance gain using orbital diversity as a possible countermeasure method.

The dashed line designates the exceedance probability versus excess attenuation, applying the theoretical model for double orbital diversity. The plots reveal that the theoretical model approximates quite well the measured values. For example, at 0.1% exceedance probability, the absolute difference between the measured and the theoretical attenuation is 0.04 dB. Higher divergences are observed for attenuation levels greater than 12 dB, although with lower outage values, as it is apparent in Fig. 7. The presented results validate the accuracy of the theoretical model for double orbital diversity, which can be exploited as a useful mathematical tool for robust outage estimations even when measurements are not available at the areas of interest. A different set of measurements at greater angular separations would probably provide a better understanding of the effectiveness of this technique, as suggested by [31]. Given also the fact that the KaSAT receiver has a lower measurement dynamic range, limits the extent of this evaluation to exceedance probabilities only higher than 0.01%, while it is expected that at lower probabilities the gain could be significantly higher.

Conclusion

This paper assessed the performance of site and orbital diversity in Cyprus and Greece at Ka- and Q-bands. Locally measured rainfall rate data were leveraged for the calculation of the statistical properties, which were used as inputs in the introduced theoretical model. Where data were not available, the rainfall statistics were determined by the ITU rain maps. The findings demonstrated that implementing double and triple site or orbital diversity schemes significantly reduced outage duration. Higher outage improvements are encountered in Cyprus, compared with Greece, especially at Ka-band. Furthermore, the analysis showed that for highly reliable links at Q-band, triple site diversity seems a practical and effective approach. Significant outage improvements were

https://doi.org/10.1017/S1759078726102852 Published online by Cambridge University Press

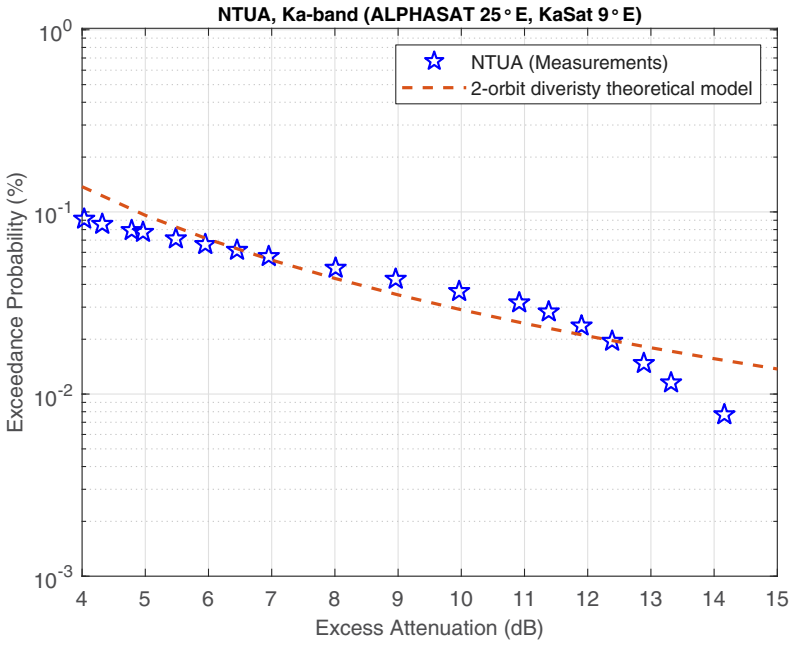

Figure 7. Orbital diversity evaluation at Ka-band comparing measurements and theoretical model.

also obtained by applying orbital diversity, although with inferior performance compared with site diversity. Generally, double-site diversity meets the requirements for convenient service availability at Ka-band. However, at Q-band, the fade margin expectations are above 10–12 dB, making triple site diversity indispensable. Finally, the joint measured attenuation values for a dual orbital diversity experimental scenario in Athens, Greece, were well approximated by the introduced theoretical model with small discrepancies. The results corroborated that the theoretical model can be well exploited for reliable outage estimations and advanced fade mitigation techniques.

In future work, the authors intend to evaluate collected measured data from beacons at the two teleport locations in Cyprus, analyze the rain statistics and attenuation, and assess the performance of site and orbital diversity scenarios in the island, having a further comparison with Greece. They also intend to apply diversity techniques for non-geostationary satellites operating above 10 GHz.

Acknowledgements. This work was funded by the European Space Agency (ESA), Contract No. 4000141612/23/NL/SC/rp. with Cyprus Telecommunications Authority (Cyta).

Competing interests. The authors declare none.

References

1. **Moraitis N, Papafragkakis AZ, Panagopoulos AD, Ioannides P, Christoforou N, Agrotis C and Alexandrou S**, (2025) *Site diversity reception performance evaluation in Cyprus at Ka- and Q-band for high throughput satellite systems. 19th European Conf. Antennas Propag. (EuCAP)*. Stockholm, Sweden.
2. **Ventouras S, Martellucci A, Reeves R, Rumi E, Fontan FP, Machado F, Pastoriza V, Rocha A, Mota S, Jorge F and Panagopoulos AD** (2019) Assessment of spatial and temporal properties of Ka/Q-band Earth-space radio channel across Europe using Alphasat Aldo Paraboni payload. *International Journal of Satellite Communications and Networking* **37**, 477–501.
3. **Kelmendi A, Csurgai-Horváth L, Svigelj A, Mohorcic M, Javornik T and Hrovat A** (2023) Site diversity experiment in Q-band satellite communications in Slovenia and Hungary. *IEEE Antennas and Wireless Propagation Letters* **22**, 1967–1971.
4. **Monvoisin J-P, V Vaissiére, L Castanet and X Boulagner** (2024). Long-term site diversity experimental campaigns in south of France at Ka-band IEEE Int. Symp. Antennas Propag. ITNC-USNC-URSI Radio Sci. Meeting, Florence, Italy.
5. **Cano J, Israel J and Feral L** (2025) AIRIS2: A smart gateway diversity algorithm for very high-throughput satellite systems. *IEEE Wireless Communications Letters* **14**, 2189–2193.
6. **Pérez-Fontán F, Pastoriza-Santos V and Machado F** (2025) A stochastic synthetic storm technique (S-SST) for orbit and site diversity studies. *IEEE Transactions on Antennas and Propagation* **73**, 3257–3269.
7. **Iacovelli G, Lacoste C, Lagunas E and Chatzinotas S** (2025) Ground segment design for Q/V band NGSO satellite systems via ℓ_o-norm minimization. *IEEE Wireless Communications Letters* **14**, 756–760.
8. **Maekawa Y, Shibagaki Y and Takami T** (2025) Effects of site diversity techniques on the rain attenuation in Ku-band satellite communications links according to the kind of rain fronts. *IEICE Transactions on Communications* **E108-B**, 109–119.
9. **Arapoglou P-DM, Michailidis ET, Panagopoulos AD, Kanatas AG and Prieto Cerdeira R** (2011) The land mobile earth-space channel: SISO to MIMO modeling from L to Ka-bands. *IEEE Vehicular Technology Magazine* **6**, 44–53.
10. **Panagopoulos AD, Arapoglou P-DM and Cottis PG** (2004) Satellite communications at Ku, Ka, and V bands: Propagation impairments and mitigation techniques. *IEEE Communications Surveys & Tutorials* **6**, 2–14.
11. **COST Action 255**, (2002) *Radiowave Propagation Modelling for SatCom Services at Ku-Band and Above - Final Report*. The Netherlands: ESA Publications Division.
12. **Panagopoulos AD** (2017) *Propagation Phenomena and Modeling for Fixed Satellite Systems: Evaluation of Fade Mitigation Techniques. in Radio Wave Propagation and Channel Modeling for Earth-Space Systems*. Boca Raton, FL, USA: CRC Press.
13. **Panagopoulos AD and Kanellopoulos JD** (2002) Prediction of triple-orbital diversity performance in Earth-space communication. *International Journal of Satellite Communications* **20**, 187–200.
14. **Barbaliscia F, Ravaioli G and Paraboni A** (1992) Characteristics of the spatial statistical dependence of rainfall rate over large areas. *IEEE Transactions on Antennas and Propagation* **40**, 8–12.

https://doi.org/10.1017/S1759078726102852 Published online by Cambridge University Press

15. **ITU-R P.618-14** (2023) *Propagation Data and Prediction Methods Required for the Design of Earth-Space Telecommunication Systems*. Geneva, Switzerland.
16. **Kanellopoulos JD and Koukoulas SG** (1990) Prediction of triple site diversity performance in Earth space systems. *Journal of Electromagnetic Waves and Applications* **4**, 341–358.
17. **Kanellopoulos JD, Koukoulas SG, Kolliopoulos NJ, Capsalis CN and Ventouras SG** (1990) Rain attenuation problems affecting the performance of microwave communication systems. *Annales des téléCommunications* **45**, 437–451.
18. **Kelmendi A, Kandus G, Hrovat A, Kourogiorgas CI, Panagopoulos AD, Schönhuber M, Mohorčič M and Vilhar A** (2017) Rain attenuation prediction model based on hyperbolic cosecant Copula for multiple site diversity systems in satellite communications. *IEEE Transactions on Antennas and Propagation* **65**, 4768–4779.
19. **Karagiannis GA, Panagopoulos AD and Kanellopoulos JD** (2012) Multidimensional rain attenuation stochastic dynamic modeling: Application to Earth-space diversity systems. *IEEE Transactions on Antennas and Propagation* **60**, 5400–5411.
20. **Matricciani E** (1983) An orbital diversity model for Earth to space links under rain and comparisons with site diversity. *Radio Science* **18**, 583–588.
21. **Flávio J, Perez-Fontan F, Jorge F, Mota S and Rocha A** (2017) *Joint results of the Aveiro and Vigo Alphasat propagation campaigns. 11th European Conf. Antennas Propag. (EuCAP)*. Paris, France.
22. **Luini L, B Wioland and C Riva** (2022) Orbital and spatial diversity for next generation large NGSO satellite constellations *Microwave Mediterranean Symposium (MMS)*. Pizzo Calabro, Italy.
23. **ITU-R P.837-7** (2017) *Characteristics of Precipitation for Propagation Modelling*. Geneva, Switzerland.
24. **ITU-R P.839-4** (2013) *Rain Height Model for Prediction Methods*. Geneva, Switzerland.
25. **Crane RK** (1996) *Electromagnetic Wave Propagation Through Rain*. New York, USA: John Wiley & Sons.
26. **Kanellopoulos JD and Panagopoulos AD** (2001) Ice crystals and raindrop canting angle affecting the performance of a satellite system suffering from differential rain attenuation and cross-polarization. *Radio Science* **36**, 927–940.
27. **Panagopoulos AD, Livieratos SN and Kanellopoulos JD** (2002) Interference analysis applied to a double site diversity Earth-space system: Rain height effects and simple regression-derived formulas. *Radio Science* **37**, 1–9.
28. **Sakarellos VK, Skraparlis D, Panagopoulos AD and Kanellopoulos JD** (2009) Optimum placement of radio relays in millimeter-wave wireless dual-hop networks [Wireless Corner]. *IEEE Antennas and Propagation Magazine* **51**, 190–199.
29. **Emiliani LD, Luini L and Capsoni C** (2008) Extension of ITU-R method for conversion of rain rate statistics from various integration times to one minute. *Electronics Letters* **44**, 557–558.
30. **Matricciani E** (1998) Diurnal distribution of rain attenuation in communication and broadcasting satellite systems at 11.6 GHz in Italy. *IEEE Transactions on Broadcasting* **44**, 250–258.
31. **Matricciani E and Mauri M** (1995) Italsat-Olympus 20-GHz orbital diversity experiment at Spino d'Adda. *IEEE Transactions on Antennas and Propagation* **43**, 105–108.
32. **Papafragkakis AZ, Panagopoulos AD and Ventouras S** (2017) *Combined beacon and noise satellite propagation measurements using software defined radio. 11th European Conf. Antennas Propag. (EuCAP)*. Paris, France.
33. **Papafragkakis AZ, Kourogiorgas CI and Panagopoulos AD** (2019) Site-diversity Ka-band satellite propagation campaign in Attica, Greece, using Alphasat: First 2 Years' Results. *IEEE Antennas and Wireless Propagation Letters* **18**, 2115–2119.

Nektarios Moraitis received the Diploma and Ph.D. degrees in electrical and computer engineering from the National Technical University of Athens, Greece, in 1998 and 2005, respectively. He is a teaching and research associate (faculty staff) at the School of Electrical and Computer Engineering, National Technical University of Athens. He has more than 100 publications in international journals, conference proceedings, and book chapters. His current research interests include propagation for next-generation wireless communications, channel measurements, characterization, simulation, and modeling for fixed and mobile terrestrial and satellite communications systems. Dr. Moraitis has been serving as the Chair of the IEEE Vehicular Technology/Aerospace and Electronic Systems Joint Chapter, Greek Section since 2020. He is ranked in the top 200 reviewers (2022, 2024, and 2025) of the journal IEEE Transactions on Antennas and Propagation and received the Outstanding Reviewers Award 2025 of the journal IEEE Open Journal of Antennas and Propagation.

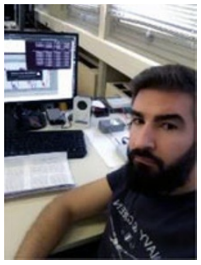

Apostolos Z. Papafragkakis received the graduate and Ph.D. degrees from the School of Electrical and Computer Engineering, National Technical University of Athens (NTUA), in 2014 and 2021, respectively. His doctoral research focused on satellite communications at high-frequency bands, with emphasis on propagation effects and software-defined radio (SDR) systems. He has participated in numerous international conferences and is the author of several peer-reviewed journal papers and technical articles. His research background includes signal processing and wireless communication systems, with hands-on experience in SDR platforms. He is a member of the Technical Chamber of Greece (TEE).

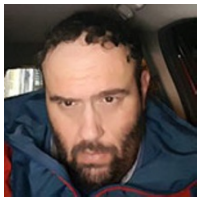

Athanasios D. Panagopoulos was born in Athens, Greece, on 26th January 1975. He received the Diploma degree (summa cum laude) in Electrical and Computer Engineering and the Ph.D. degree in Engineering from the National Technical University of Athens (NTUA), Athens, Greece, in 1997 and 2002, respectively. Since September 2021, he has been a Full Professor with NTUA. He has published more than 200 papers in international journals and IEEE transactions and more than 250 papers in conference proceedings. He has also published more than 35 book chapters in international books. His research interests include radio and optical communication systems design, wireless and satellite communications networks, and the propagation effects on communication protocols. Prof. Panagopoulos has been appointed as a Member of the Hellenic Telecommunications and Post Commission (EETT) Plenary since 2022. He is currently an Associate Editor of the ITU Journal on Future and Evolving Technologies.

https://doi.org/10.1017/S1759078726102852 Published online by Cambridge University Press

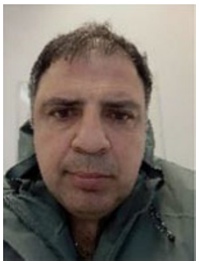

Panayiotis Ioannides received the Diploma in Electrical and Computer Engineering from the National Technical University of Athens, Greece, in 2002, and the MS degree in Electrical Engineering from Arizona State University, USA, in 2004, with research focusing on the design of smart antenna systems and algorithms. He holds an MBA degree from the University of Cyprus. For the last ten years, he has been serving as Telecommunications Engineer for Cyta's Satellite Operations, dedicated to operation, maintenance, troubleshooting, and expansion activities, including the critical Galileo Search and Rescue facilities in Cyprus, as well establishment of new projects, including financial roles and procuring processes. He also serves as Technical Administrator of Cyta's IPTV platform. For the past few years, he has been actively involved in securing and implementation of research projects on behalf of Cyta, through the Plan for European Cooperating States (PECS), designed to prepare countries to join ESA as Associate Members.

Nikolaos Christoforou is currently pursuing his Ph.D. degree at the Cyprus University of Technology. His research interests include the detection and localization of interference in GNSS networks. He holds an MBA degree from the University of Cyprus and an MSc degree in Mobile and Satellite Communications from the University of Surrey. He is currently the Head of the Radio Access Network at Cyta, having previously served for twenty years as Operations Manager for Ground Satellite Operations, where he led and contributed to the deployment of large-scale projects. During his tenure, he played a key role in the expansion of ground teleport facilities, the incorporation of operational processes, and the implementation of industry best practices, leading to international recognition of Cyta's teleport facilities. He was also actively involved in customer support, serving as a point of contact for third-level support, and contributed to commercial activities through the promotion of Cyta's satellite services.

Constantinos Agrotis holds a BEng. degree in Electrical Engineering from Stony Brook University (USA), MSc. degree in Electrical Engineering from the University of Dayton (USA), and Master's degree in Business Administration (MBA) from Cyprus International Institute of Management (CIIM). He has been working with Cyta since 1991 and is currently appointed as the manager of Teleport, which originally included three expertise areas: The Satellite Systems, the Digital TV Platforms, and the Submarine Fiber Cable Systems. He has been involved heavily as an engineer of the department in the three expertise areas leading numerous projects and has evolved as a teleport manager. His duties include among others planning, coordination, and control of development work as well as working closely with the commercial services to attract new customers. His contribution and interaction with the broader team enabled the recognition of the Cyprus Teleport as one of the most important International Hubs in the region offering quality products of technological superiority.

Sotirios Alexandrou has a Ph.D. degree in Electrical Engineering from the University of Rochester and long experience in telecommunications. He is responsible for developing and promoting Cyta's satellite services in the international market and serves as the company's coordinator in space projects. He plays a key role in efforts to establish Makarios Teleport as a major satellite gateway for operators and key customers, offering a wide range of services. Dr. Alexandrou explores synergies between satellite teleport services, broadband products, and fiber connectivity. His efforts enhance Cyta's satellite capabilities and strengthen its role as a telecommunications hub in the Eastern Mediterranean. He leads Cyta's efforts to attract major international clients and was instrumental in securing key contracts with industry leaders. He works comfortably in a demanding competitive environment with consistently solid results. His research background includes notable contributions in optoelectronics, superconducting circuits, photodetectors, and ultrafast transmission lines.

https://doi.org/10.1017/S1759078726102852 Published online by Cambridge University Press